J Mater Sci (2009) 44:227–233
DOI 10.1007/s10853-008-3082-3

Fabrication and properties of a lubrication composite coating based on poly(*p*-hydroxybenzoic acid) (PHBA)

Wang Jian · Zhao Wenzhen · Guo Chaowei

Received: 24 January 2008 / Accepted: 22 October 2008 / Published online: 27 November 2008

Abstract The present paper describes an approach for fabricating smooth, compact and homogeneous composite coatings of PHBA/PA/MoS_2 on test blocks. The tribological behaviors were tested on a ring-block machine. For the PHBA/PA 6,6/MoS_2 coating of 20 wt.% PA 6,6 and 30 wt.% MoS_2 with the thickness of 20–40 μm, the steady friction coefficient was approximately 0.04 with the lowest wear loss while sliding against AISI 1045 steel ring. The PHBA in coating was synthesized in situ at 200 °C for the first step and 260 °C for the second. The chemical structures and thermal properties of the obtained PHBA were characterized by means of Fourier transform infrared spectroscopy (FT-IR) and differential scanning calorimetry/thermogravimetry (DSC/TG). The results showed that the chemical structure of the obtained PHBA was identical to that of the commercial PHBA powder despite that the decomposition temperature and the crystal transition temperature of the former were approximately 10–20 °C lower than that of the latter. The influence of nominal pressure and sliding velocity on the friction coefficient (μ) and wear volume loss of the coatings was investigated. The results displayed that μ increased with the increase of sliding velocity, while it decreased when the nominal pressure was increased. For the volume loss, it increased with both the increase of speed and pressure.

W. Jian (✉) · Z. Wenzhen · G. Chaowei
State Key Laboratory for Mechanical Behavior of Materials, School of Material Science and Engineering, Xi'an Jiaotong University, Xi'an 710049, China
e-mail: yjswangjian@stu.xjtu.edu.cn; yjswangjian@yahoo.com.cn

W. Jian
School of Chemistry & Chemical Engineering, Yangzhou University, Yangzhou 225002, China

Abbreviations

PHBA	Poly(*p*-hydroxybenzoic acid)
T_d	Decomposition temperature
T_c	Crystal transition temperature
T_m	Melting temperature
OM	Optical microscope
PA 6,6	Polyamide 6,6
p-ABA	*p*-acetoxybenzoic acid
p-HBA	*p*-hydroxybenzoic acid
THF	Tetrahydrofuran
FT-IR	Fourier transform infrared spectroscopy
T_g	Glass transition temperature
DSC	Differential scanning calorimetry
TGA	Thermogravity analysis
$\bar{D}_p$	Mean polymerization degree
$\bar{M}_w$	Mean relative molecular weight

Introduction

PHBA has a series of advantages such as outstanding self-lubrication, excellent thermoconductivity, and prominent thermostability in air among all polymers. PHBA has no T_m or T_g and only shows a crystal transition temperature T_c approximately to 325–360 °C and decomposes at 535 °C [1, 2]. Economy et al. [3] proved that its T_c was characteristics of a plastic crystal or a highly ordered nematic phase transition for only low molecular weight samples of the homopolymer. Mathew et al. [4] reported a kinetic study of the synthesis of PHBA by melt step growth and found that the polycondensations obey second-order kinetics irrespective of whether the reaction was catalyzed or uncatalyzed.

PHBA can ensure a long service life beneath 315 °C and a transitory one at 370–425 °C. The sliding friction coefficient of the molded parts of PHBA might be as low as 0.32–0.16. Nevertheless, PHBA has a shortcoming of poor workability because it is infusible at any temperature and unsolvable in any solvent. In recent years, only molded PHBA/PTFE parts fabricated by cool pressure sintering or compression molding at a temperature in excess of 400 °C have been applied for self-lubricants [5]. However, to the author's knowledge, no work yet has been reported in the literature concerning a method similar to ours for preparing the PHBA-based lubrication coatings through synthesizing PHBA in situ and forming coatings synchronously, which exhibit potential applications in aviation and spaceflight.

PA 6,6, with a T_m of 253 °C, may serve as thermoplastics with good mechanical performance at elevated temperatures. It also exhibits good resistance to friction and wear under rigorous circumstances [6]. More importantly, PA 6,6 powder can form thin films readily on metals. This meets our need to improve the formation of thin film on substrate by doping PA 6,6 in PHBA-based coatings.

From the perspective of chemical interactions, PA 6,6 and PHBA are both polar molecules. H atoms in the N–H bonds of a PA 6,6 molecular chain tend to form hydrogen bonds with O atoms of C=O groups in a PHBA molecular chain. On the other hand, Fe and Ni can combine with active nonmetal such as O, S, N, Cl, etc., by the forming ionic bonds. Meanwhile, on the base of electron distribution of Fe (II) and Fe (III) and Ni (II), they all own void atomic orbit *d* so they can accept both the lone electron pairs of N, O atom in PHBA and PA 6,6 and π electrons of benzene ring in PHBA. There exist complex bonds between Fe (II, III), Ni (II), and PHBA and PA 6,6. The composite coating can tightly attach to the Ni substrate and so does the transfer film formed during the wear process to the mating metal to increase the durability of the tribological system (Fig. 1).

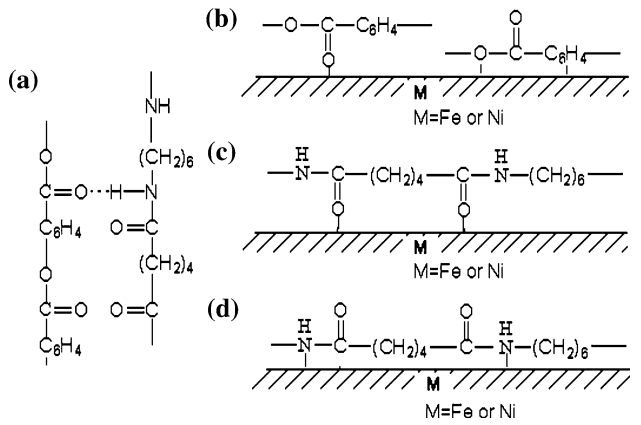

Fig. 1 Schematic presentation of intermolecular H-bond between PHBA-PA 6,6 (**a**) and the interaction of Fe, Ni with PHBA/PA 6,6 via ionic bond and/or complex bonds (**b**, **c**, **d**)

Experimental

Materials

p-ABA was prepared by refluxing *p*-HBA with a 10% (mole) excess of acetic anhydride at 130–150 °C [5, 6]. The PHBA powder (75 μm) for comparison use was presented by Chenguang Research Institute of Chemical Industry, China. MoS_2 colloidal powder (1–3 μm), PA 6,6 powder (80–120 grids), and other chemical reagents were purchased from Shanghai Chemical Reagent Research Institute, China.

Experiments & instruments

The test blocks used for fabricating coatings were made of AISI 1045 steel. Before coating, the test blocks were cut into the dimensions of 31 × 7 × 6 mm^3. A layer of Ni (20 μm) was then deposited electrically on each block in advance to increase the wear resistance. Afterwards, the surfaces of the test blocks (the layer of Ni) were polished via 1,200 grid emery paper and washed ultrasonically for 1 min in acetone. Each test block was brushed on its Ni-plated surface with a slurry (0.3 g/L) which was obtained by adding the powder mixture of PA 6,6 and MoS_2 into the solution of *p*-ABA in tetrahydrofuran. In the first step, the synthesis of PHBA was carried out at 200 °C for 2 h in a salt bath (NaCl). In the second step, the reaction mixture was heated to 260 °C and held at that temperature for 4 h. The fabrication of PHBA-based coatings was performed synchronously. Each step was under the protection of N_2 (99.9%).

In order to inhibit the sublimation of *p*-ABA, a specific system of two reactors was designed for preparing the PHBA or PHBA-based composite coatings. The inner reactor (Φ 32 × 41 mm^2) was modified from a beaker (Fig. 2), which was clasped by two steel plates (60 × 60 × 5 mm^3) with nuts to tight them. The interface between the steel plate and the beaker was sealed with fluorine rubber. The coated steel test blocks (substrate) were placed above a large quantity of *p*-ABA or mixture of *p*-ABA/PA 6,6 or *p*-ABA/PA 6,6/MoS_2 to reduce the loss of *p*-ABA owing to its inevitable sublimation as possible. For each case, the composition of the coating was the same as that of the mixture coexisted in the inner reactor, namely, content of every ingredient in coating was equivalent to that in the mixture. So the sublimation of *p*-ABA (a little amount) in coating on test block would be inhibited by sublimation of *p*-ABA (a large amount) in the mixture according to the theory of *Equilibrium Shift*. Before heating, the reactor was filled with N_2 and vacuumed (0.04 MPa) at room temperature. The same process was repeated three times. The whole inner reactor was sealed tightly and then placed into another larger (outer) reactor (Φ 140 × 135 mm^2) with an inlet and an outlet of N_2 and a

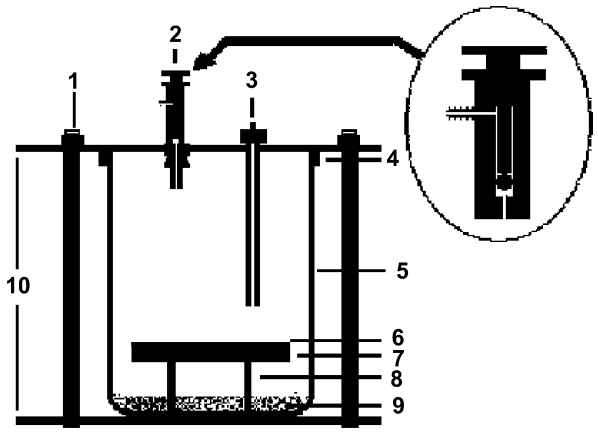

1-nut
2-outlet for vacuum
3-inlet for N2
4-fluorine rubber
5-beaker
6-composite coating
7-test block
8-support
9-mixture of PHBA, PA6,6 and MoS2
10-metal plate

Fig. 2 The inner reactor for preparing PHBA-PA-MoS_2 composite coating

heating controlling system. Especially, in order to avoid the sublimation of *p*-ABA, vacuuming the inner reactor was not suitable for preparing PHBA at the second step of the polymerization process (See Eq. 3 in section "Principles for synthesizing PHBA") in our research.

$\bar{D}_p$ or $\bar{M}_w$ of the prepared PHBA and the commercial PHBA were determined referring to the literature [4]. The infrared spectra of all samples were recorded on a Shimadzu FTIR-8400S spectrophotometer with PHBA specimens compressed in KBr disks. DSC/TG curves were obtained on a NETZSH STA 449C interfaced with a thermal analysis data station. Samples weighing about 10 mg were heated under nitrogen from room temperature to 600 °C with a rate of 10 °C/min. The sliding wear tests were carried out on a block-on-ring test machine (type: MM-200, made in Xuanhua, China) under ambient conditions of temperature and humidity with normal load 50 N and sliding velocity 0.42 m/s for 1,800 s. An AISI 1045 steel test ring of Φ 40 × 12 mm^2 was polished with an abrasive paper (Al_2O_3, 180#) to a roughness of 1.2 μm Ra. Before each test, the wear track on the test ring was refreshed by pressing a T 200# metallurgical abrasive paper for 2 min and washing three times with acetone to ensure the same initial condition. The wear volume loss was obtained by the calculation from the depth and width of the wear track (Fig. 3). The average friction coefficient and wear volume loss of three replicate tests for each specimen were reported as results in this study. Thickness of all obtained composite coatings ranged from 20 to 40 μm under OM.

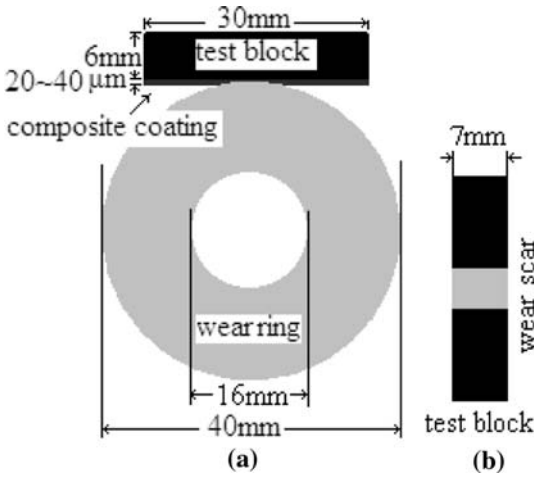

Fig. 3 Schematic illustration of friction between the test block and wear ring (**a**) and the wear scar (**b**)

Results and discussions

Principles for synthesizing PHBA

p-ABA was prepared from *p*-HBA according to the Eq. 1 [5, 6]

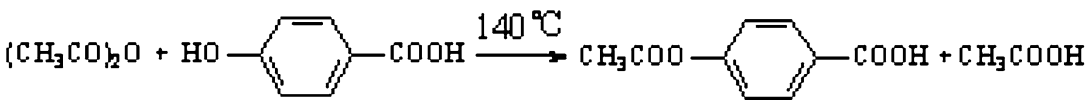

(1)

Then PHBA was polymerized from *p*-ABA according to the Eqs. 2 and 3

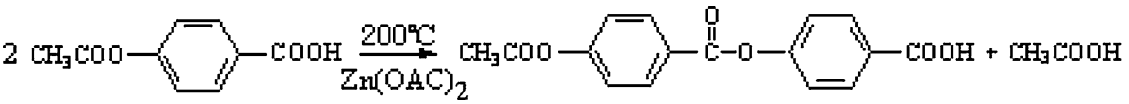

(2)

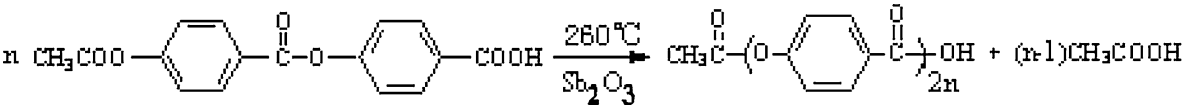

(3)

Conditions for preparing PHBA/PA/MoS_2 coating

During the synthesis of PHBA, 200 °C for the first step and 260 °C for the second step were the optimal conditions in this research. The temperatures were about 100 °C lower than that reported [8] elsewhere. One reason is that a PHBA homopolymer of a lower $\bar{D}_p$, rather than a higher one, is beneficial to a low friction coefficient and wear volume loss. Meanwhile, bubble-like defects were observed on the surface of the obtained coatings over 260 °C because bubbles of CH_3COOH, the by-product of the reaction, were difficult to be excluded rapidly and thoroughly in the absence of stirring in this study.

Structure of the obtained PHBA

The infrared spectra testify to the prepared PHBA concerning the identities of absorption bands (Fig. 4) for the synthesized product and the commercial PHBA powder. Please note that the PHBA for FT-IR and DSC/TGA analysis was solely synthesized under the same conditions as that for obtaining PHBA-based coatings. The both spectra showed a band at 1,741 cm^{-1} due to the C=O stretching, and a 1,380 cm^{-1} band due to the C–H symmetrical deformation in $–CH_3$. However, a weak band at 1,680 cm^{-1} in spectrum (Fig. 4a) was indicative of the residual end group, COOH, of the prepared PHBA, while for commercial PHBA powder, no discernible absorption peak could be found at this position. That is, the ratio of COOH in the prepared PHBA molecular chains was higher than that in the PHBA chains for comparison. This might be interpreted by the fact that the $\bar{D}_p$ of the prepared OB was relatively lower than that of the commercial PHBA due to the lower temperature employed in our study. The $\bar{M}_w$ of the prepared PHBA was about 3300–3500, and its $\bar{D}_p$ was approximately 33–35. For the commercial PHBA, its $\bar{M}_w$ was determined as 8,500–9,100, the $\bar{D}_p$ was 85–91 [4, 9, 10].

TGA and DSC analysis of PHBA

The decomposition temperature (T_d) of the prepared PHBA was 512.5 °C; for the PHBA powder, 535.5 °C (Fig. 5). The DSC thermograms exhibit distinct endotherms, depicting the highly crystalline nature of PHBA. The crystal transition temperature (T_c) of the prepared PHBA was 322 °C; for the PHBA powder, 337 °C. The T_d and T_c of the prepared PHBA are lower than that of the commercial PHBA powder [11]. This is in agreement with the relatively lower $\bar{D}_p$ of the prepared PHBA due to the lower reaction temperature. Anticipating from the starting temperature for decomposition (~350 °C), the prepared PHBA in our study is suitable to be used under 300 °C.

A PHBA single crystal of lower $\bar{D}_p$ (<39) will undergo a transition into a nematic crystal under shear stress above T_c. However, a PHBA sample of high molecular weight ($\bar{D}_p > 39$) will not exhibit any tendency to flow above T_c even under a higher localized shear [11]. This may well be due to the fact that the formation of a nematic phase requires that sufficient force be applied to overcome the dipolar interactions between chains. For the low molecular weight PHBA, there are few ester units contributing to the stabilization of the structure and the dipolar interactions within it are easy to overcome by the applied shear. With the increase in the molecular weight, the shearing process becomes increasingly difficult due to the increasing number of dipolar interactions until finally the polymer becomes intractable.

The flow or orientation of PHBA molecular chains under shear is facilitated by the presence of lower molecular weight species. In this research, lower temperatures

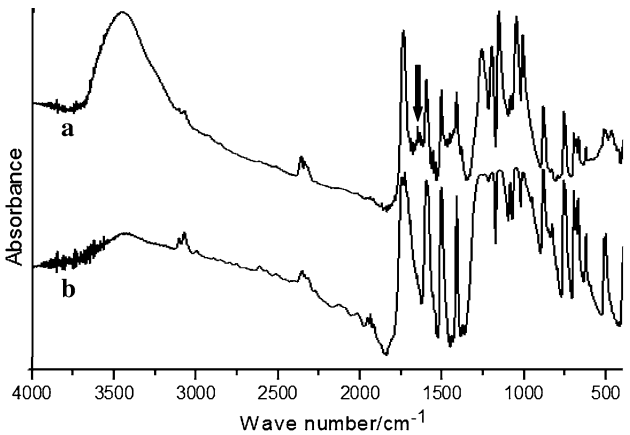

Fig. 4 IR spectrum of the PHBA synthesized (a) and IR spectrum of the PHBA commercially available (b)

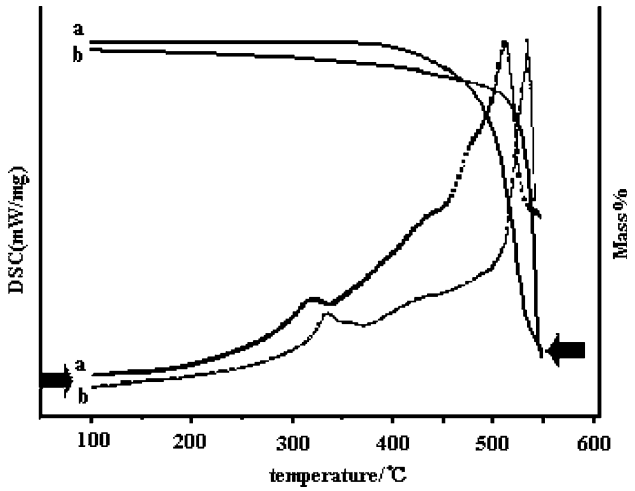

Fig. 5 TGA and DSC spectrum of the PHBA self-prepared (a) and the commercially available (b)

were employed to obtain a PHBA of both a moderate T_c and $\bar{D}_p$. This will result in a low friction coefficient as well as a low wear loss for the lubrication coating by plastic crystal transition and sufficient loadability.

Friction and wear behavior of the PHBA-PA-MoS_2 composite coating

The fabricated composite coatings exhibited superb tribological characteristics. The friction coefficient (Fig. 6) dropped evidently with increasing MoS_2 content of the prepared composite coating. A steady friction coefficient less than 0.04 was achieved for the MoS_2-50 wt.% coating. However, the wear volume loss rose remarkably when the MoS_2 content was higher than 30 wt.%. The reasons for this phenomenon may be that when MoS_2 content is higher than a critical value (e.g. 30 wt.% in this paper), the adhesion among the coating constituents or of the coating to substrate will become weaker. This will make MoS_2 cast off the coating, and/or result in the gradual and progressive wear through the bulk of the coating or even the delamination of coating from substrate due to the origination and evolution of faults/microcracks at the interface or within the coating when the load and shear stress go beyond the film's yield strength. The friction coefficient was 0.043 for the coating of PHBA (50 wt.%)/PA 6,6 (20 wt.%)/MoS_2 (30 wt.%) with the lowest wear loss during sliding against the counterpart.

The reduction of friction in a composite coating may be ascribed to its intrinsic self-lubricity at the tribological surface. During sliding, chains of lower $\bar{M}_w$ PHBA ($\bar{D}_p < 39$) undergoes a transition into nematic phase, and one might expect to see flow of these chains under shear stress when the local temperature rises above its T_c. Other PHBA chains, especially those at the edges of PHBA particles, tend to orient to the direction of the shear stress due to the breakdown of ester–ester dipole interaction between the double helices [4]. Meanwhile, PA 6,6 (T_m 253 °C) possesses good friction and wear performances due to its linear flexible molecular chain which leads to better rheology and orientation in the sliding direction [14]. All these factors plus low-shear layered MoS_2 as solid lubricant undoubtedly contribute to the low friction coefficients [15] (Fig. 7).

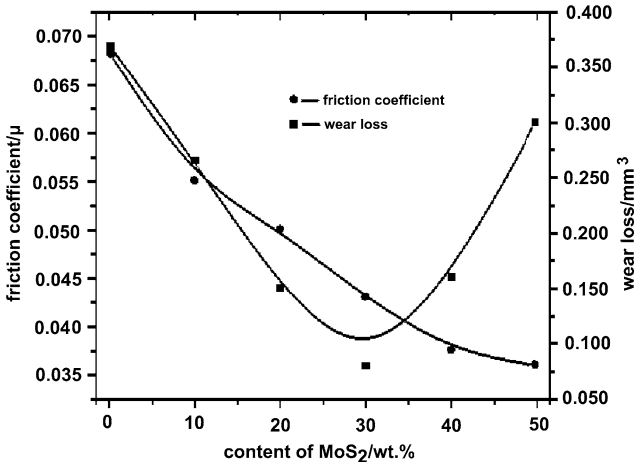

Fig. 6 Friction coefficient and wear volume loss of PHBA-PA-MoS_2 coating of various content of MoS_2

Furthermore, the decrease of the friction coefficient of a PHBA-based composite coating is also attributed to the formation of a transfer film on the counterface, which consists of the wear particles of the coating components and the products of tribo-chemical reactions (e.g. decomposing, crosslinking of polymer chains, and the reaction of MoS_2 with Fe) [16, 17]. Some extent of reduction in the friction coefficient will be attainable if the transfer film is molecularly smooth with low shear strength. Besides, the bonding of the transfer film is enhanced by tribo-chemical reactions, which thus reduces the wear rate by protecting the coating surface from aggressive damage of hard metal asperities. Meanwhile, a back transfer film is simultaneously developed on the composite by transferring from the counterface into the coating. The transfer film on the metal surface and the back transfer film on the coating are vital for a low friction coefficient and a long service life of the whole tribo-system [18].

Influence of the nominal pressure P and sliding velocity V on the tribological behaviors of the composite coating

The friction coefficient μ and wear volume loss of the coatings appeared strongly to be influenced by the combined action of P and V during contact process. μ increased with the increase of V, while it decreased when increasing P. For the volume loss, it increased with both the increase of P and V.

At a constant V, μ decreased linearly with the increase of nominal pressure (Fig. 8). This is plausible because we could only obtain an incomplete transfer film on the surface of the wear ring under a low load. With increasing P, stress at the interface between the contact area increased and the plastic deformation and shear flow enhanced. This sped the production of debris of the coating and a smooth, uniform and consecutive transfer film then grew up on the surface of the mating metal. This transfer film reduces the friction coefficient by preventing the direct contact between the coating and the metal.

On the other hand, μ increased slightly when the speed rose from 0.42 to 0.84 m/s under a constant load. The reasons for this might be that the transfer film on the surface of the friction pair became more incomplete due to the fatigue fracture of certain molecular chains of the

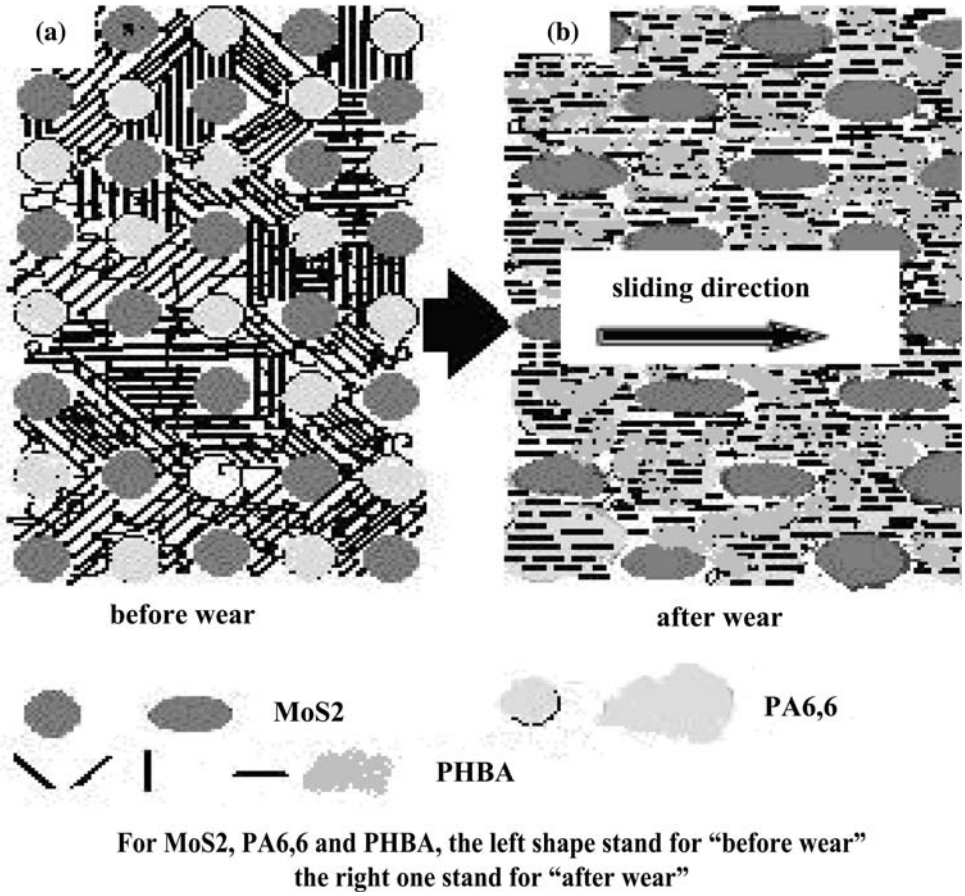

Fig. 7 Schematic illustration of lubrication principle of PHBA-PA-MoS_2 coating

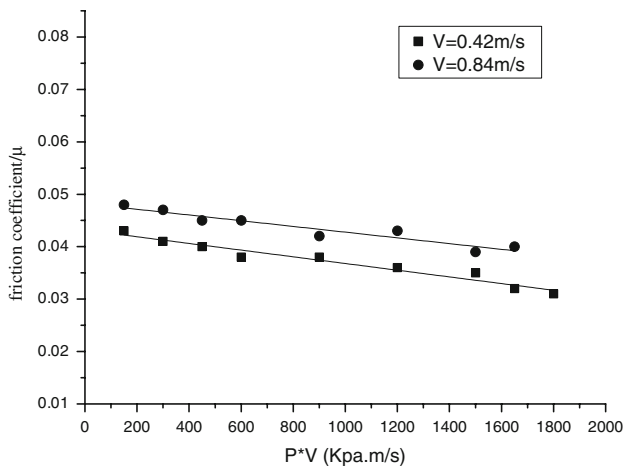

Fig. 8 Influence of pressure and velocity on the friction coefficient of the composite coatings

polymer, because the impact frequency of the asperities of metal to the coating rose when V was increased. Meanwhile, the ascending of temperature on the surface of the coating owing to the friction-induced heat resulted in the severe plastic deformation and adhesive wear at a higher V. Then, the adhesion and plough were enhanced with the increase of the real contact area A_r. Consequently, the friction force F and μ increased with increase in the sliding speed [19].

Under a low $P * V$, the wear volume loss of a composite coating was low while sliding against the counterpart, which is because only elastic deformation on the coating without hysteresis occurs and the real contact area is relatively low. However, a rapid increase was observed while increasing the value of $P * V$, especially when PV values exceed 900 Kpa m/s (Fig. 9). In the first place, adhesive wear will be enhanced with increasing nominal load because asperities of the mating face will cut in the coating more deeply and the A_r will increase to be close to the nominal contact area. In the meanwhile, at a higher speed and temperature, the higher frequency and deformation rate as well as the thermally activated fracture will cause the wear volume loss to grow rapidly. In the second place, the collapse of the wear resistance of the coating is associated with the internal instability processes originating from the rheological modifications when the instantaneous flash temperature approaches and surpasses the T_m of PA 6,6 or even the T_c of PHBA. That is, melting of PA 6,6 and shear flow of PHBA will occur as the local temperature rises while increasing P or V. Moreover, PHBA has as a high

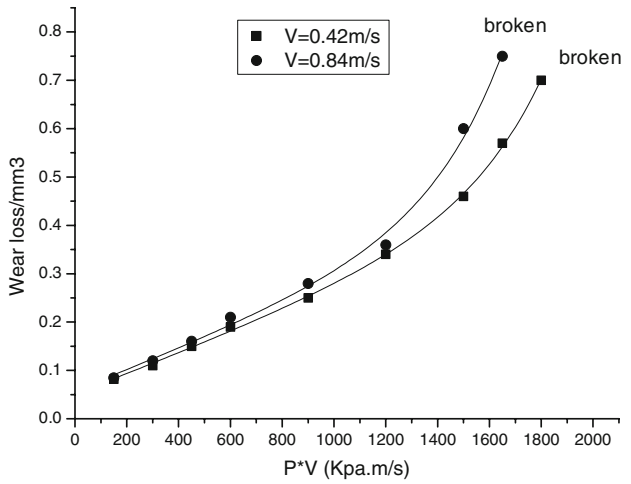

Fig. 9 Influence of pressure and velocity on the wear volume loss of the composite coatings

heat transfer coefficient as that of the iron, so it will transfer the friction heat readily from the surface to the subsurface and even the bulk of the coating. Then temperature grade will form within the area from the surface to the subsurface and bulk of the coating. The shear deformation will then be enhanced within the surface and subsurface. The fatigue wear resulting from repeated sliding, on the other hand, will enhance the nucleation and evolution of the micro-crack at the interface and eventually lead to a severe wear by transferring a large proportion of the coating to the metal [20].

Conclusions

(1) The prepared PHBA exhibited an identical structure to that of the commercial PHBA powder. However, the former displayed a relatively higher percentage of –COOH due to the relatively lower polymerization degree under the conditions employed in our research.

(2) T_d and T_c of the prepared PHBA were 512.5 °C and 322 °C, respectively, which makes it possible to use this kind of PHBA under 300 °C.

(3) The friction coefficient μ of PHBA (30 wt.%)/PA 6,6 (20 wt.%)/MoS_2 (30 wt.%) with the thickness of 20–40 μm was approximated to be 0.04 when sliding against the friction counterpart.

(4) The friction coefficient μ and the wear volume loss of the coating were strongly influenced by the sliding velocity V and the nominal pressure P during contact process. μ increased with the increase of V, while it decreased when increasing the P. For the volume loss, it increased with both the increase of P and V.

References

1. Gilkey R, Caldwell JR (1959) J Appl Polym Sci 2:198
2. Economy J, Storm RS (1976) J PolyM Sci Polym Chem Ed 14:2207
3. Economy J, Volksen J, Viney J et al (1988) Macromolecules 21:2777
4. Mathew J, Bahuleka RV, Ghadage RS et al (1992) Macromolecules 25:7338
5. Chen EQ (2002) Eng Plast Appl 30(8):57 (in Chinese)
6. Meng YZ, Tjong SC (1999) Polymer 40:2711
7. Samyn P, Baets PD, Schoukens G et al (2007) Wear 262:1433
8. Shaban H, Al-Sarawi MA, Behbehane A et al (2001) Eur Polym J 37:1115
9. Ning YC (2000) Structure identification of organic compound and organic spectroscopy, 2nd edn. Chinese Science Press, Beijing
10. Kimura K, Horii T, Yamashita Y (2003) J Polym Sci Part A: Polym Chem 41:3275
11. Tosaka M, Yamakawa M (1999) Microsc Res Tech 46:325
12. Habenschuss A, Varma-Nair M, Varma-Nair YK et al (2006) Polymer 47:2369
13. Lukasheva NV, Lukasheva A, Mosell T et al (1994) Macromolecules 27:4726
14. Kukureka SN, Hooke CJ, Rao M et al (1999) Tribol Int 32:107
15. Spalvins T (1987) J Vac Sci Technol A 5:212
16. Furlong O, Gao F, Kotvis P (2006) Tribol Int. http://www.sciencedirect.com. Accessed 12 Jul 2006
17. Novotny VJ, Pan XH, Bhatia CS (1994) J Vac Sci Technol A 12:2879
18. Samyn P, Samyn G (2006) Tribol Int 39:575
19. Bassani R, Levita G, Meozzi M et al (2001) Wear 247:125
20. Thomas Φ, Tom L, Bent T et al (2008) Wear 265:203